Topological Fermi Liquids from Coulomb Interactions in the Doped Honeycomb Lattice

Eduardo V. Castro, Adolfo G. Grushin, Belén Valenzuela, María A. H. Vozmediano, Alberto Cortijo, and Fernando de Juan

Topological Fermi liquids from Coulomb interactions in the doped Honeycomb lattice

Eduardo V. Castro, Adolfo G. Grushin, Belén Valenzuela, and María A. H. Vozmediano

Instituto de Ciencia de Materiales de Madrid,
CSIC, Cantoblanco, E-28049 Madrid, Spain.

Alberto Cortijo

Departamento de Física Teórica, Universidad Autónoma de Madrid, E-28049, Madrid, Spain

Fernando de Juan

Department of Physics, Indiana University, Bloomington, IN 47405, USA

(Dated: July 27, 2011)

We propose a simple method for obtaining time reversal symmetry ($\mathcal{T}$) broken phases in simple lattice models based on enlarging the unit cell. As an example we study the Honeycomb lattice with nearest neighbors hopping and a local nearest neighbor Coulomb interaction V. We show that when the unit cell is enlarged to host six atoms that permits Kekulé distortions, self-consistent currents spontaneously form creating non trivial magnetic configurations with total zero flux at high electron densities. A very rich phase diagram is obtained within a variational mean field approach that includes metallic phases with broken time reversal symmetry ($\mathcal{T}$). The predominant ($\mathcal{T}$) breaking configuration is an anomalous Hall phase, a realization of a topological Fermi liquid.

Introduction.— Topological matter is one of the most exciting subjects in today's condensed matter physics. The new states of matter have developed after the recognition of a different phase transition pattern not based on symmetry [3] inspired by the physics of the quantum Hall effect [1] and the anomalous Hall (AH) effect [2]. The possibility of getting a Hall conductivity or Landau levels without external magnetic fields [4, 5] has given rise to new areas of research and associated new materials as the topological insulators [6] and the even more interesting topological metals [7]. These systems allow the realization of beautiful fundamental ideas shared by different branches of physics like charge fractionalization or Majorana fermions [8, 9].
The interplay of the underlying lattice and the electronic interactions plays a very important role in the physics of these systems. In the topological metals time reversal symmetry ($\mathcal{T}$) breaking without a magnetic field is the key ingredient, which can be realized through current (or bond) ordering: the electrons spontaneously form current loops, which interact among themselves in such a way that the state is self-consistently maintained. These phases were discussed in other contexts in [10–13]. One of the earliest examples of this behavior is due to Haldane [4] who obtained a $\mathcal{T}$ broken state in a tight binding model in the Honeycomb lattice with complex values of the next to nearest neighbors hopping parameters. Ever since, the search for realization of $\mathcal{T}$ broken phases in lattice models has been very intense in the literature, the proposed models usually involving tight binding electrons with hopping beyond the nearest neighbors as in the original Haldane model, or very elaborated lattice structures as the Kagomé or pyroclore. More recently the effort

is changed to obtain these phases from interactions in more physically realizable models. There again previous examples involve next to nearest neighbor interactions, hoppings, or complicated lattice structures [14–18].

In this work we propose a very simple way to get $\mathcal{T}$ broken phases from interactions in standard physically existing crystal lattices based on enlarging the unit cell. In particular we consider a nearest neighbor tight binding model with nearest neighbor Coulomb interaction in the Honeycomb lattice and show that $\mathcal{T}$ broken phases exist as a stable ground state. The procedure can be applied to other standard lattices that can be physically realized either as existing materials or in optical lattices. The $\mathcal{T}$ broken phases found in this work provide a simple realization of the topological Fermi liquids described in [7, 19].

The model.—Guided by previous works and searching for renormalized hoppings of the type discussed in the original reference [4] we consider spinless fermions in the Honeycomb lattice with an extended Hubbard Hamiltonian that reads

$$H = -t \sum_{\mathbf{r},\boldsymbol{\delta}} a_{\mathbf{r}}^{\dagger} b_{\mathbf{r}+\boldsymbol{\delta}} \; + \; V \sum_{\mathbf{r},\boldsymbol{\delta}} a_{\mathbf{r}}^{\dagger} a_{\mathbf{r}} b_{\mathbf{r}+\boldsymbol{\delta}}^{\dagger} b_{\mathbf{r}+\boldsymbol{\delta}} \; + \; h.c. \; , \quad (1)$$

where t is the nearest neighbor hopping and V the nearest neighbor Coulomb repulsion. We use standard notation where $a_{\mathbf{r}}$ ($b_{\mathbf{r}}$) annihilates an electron at position $\mathbf{r}$ in sublattice A (B). The two inequivalent sublattices A and B are depicted in Fig. 1(a), along with the basis vectors $\mathbf{a}_{1,2}$. The vectors $\boldsymbol{\delta}$ refer to the three vectors connecting nearest neighbor sites, as shown in Fig. 1(a). To allow for $\mathcal{T}$ broken phases as mean field solutions we use an enlarged unit cell, containing six atoms, which also permits Kekulé type distortion as shown in Fig. 1(b): The
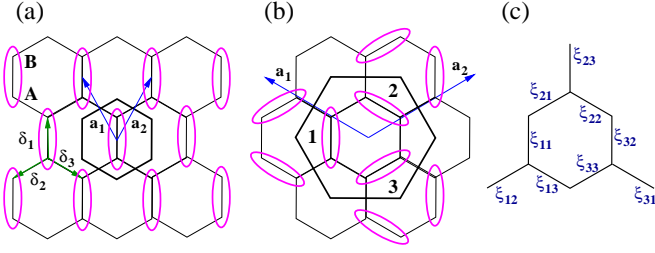
FIG. 1: (color online). (a) Two-atom unit cell and example of uniaxial distortion. The links enclosed by a circle are bigger (or smaller) than the rest. (b) Six atom unit cell and Kekulé distortion, allowed in the enlarged unit cell. (c) A pictorial representation of the nine complex order parameters considered in this work in the mean field decoupling of the Hamiltonian.
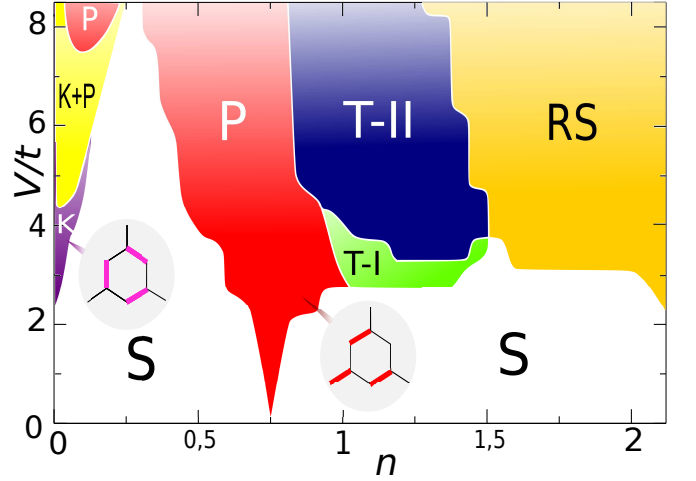

FIG. 2: (color online). Mean field phase diagram. Legend: (S) symmetric phase, i.e. bare graphene with a uniform renormalization of the hopping; (K) Kekulé distortion with hopping renormalization as shown in the inset; (P) Pomeranchuk distortion of the Fermi surface and hopping renormalization as shown in the inset; (K+P) coexistence of Kekule and Pomeranchuk distortions; (T-I) and (T-II) $\mathcal{T}$ broken phases discussed at length in the text; (RS) broken symmetry state with real hopping parameters, the distortion is neither Kekulé type nor Pomeranchuk (reduced symmetry).

links enclosed by a circle represent real values of the hopping parameter bigger (or smaller) than the others. The basis vectors of the enlarged cell in real space are $\mathbf{a}_1 = \frac{3a}{2}(-\sqrt{3}, 1)$ and $\mathbf{a}_2 = \frac{3a}{2}(\sqrt{3}, 1)$, and the respective unit cell vectors in reciprocal space are $\mathbf{b}_1 = \frac{2\pi}{3\sqrt{3}a}(-1, \sqrt{3})$ and $\mathbf{b}_2 = \frac{2\pi}{3\sqrt{3}a}(1, \sqrt{3})$. This gives rise to a tight binding model whose wave function is a six component spinor of the form $\psi_{\mathbf{k}}^\dagger = [a_1^\dagger(\mathbf{k}), b_1^\dagger(\mathbf{k}), a_2^\dagger(\mathbf{k}), b_2^\dagger(\mathbf{k}), a_3^\dagger(\mathbf{k}), b_3^\dagger(\mathbf{k})]$.

Since we are interested in the electronic phases with broken $\mathcal{T}$ we do not consider for the time being charge ordered phases. Under these conditions the most general mean field Hamiltonian depends on nine complex parameters ξ_{ij} which can be grouped in a 3×3 matrix, and that can be shown to be k−independent. The mean field equations can be written in terms of the mean field averages of the form $\langle b_j^\dagger(\mathbf{k}) a_i(\mathbf{k}) \rangle_{MF}$ as

$$\xi_{ij} = -\frac{2}{N} \sum_{\mathbf{k}} \gamma_{\mathbf{k}}^{ij} \langle b_j^\dagger(\mathbf{k}) a_i(\mathbf{k}) \rangle_{MF}, \qquad (2)$$

where N is the number of unit cells, $\gamma_{\mathbf{k}}$ is a 3×3 matrix given by

$$\gamma_{\mathbf{k}} = \begin{bmatrix} 1 & e^{-i\mathbf{a}_2 \cdot \mathbf{k}} & 1 \\ 1 & 1 & e^{i(\mathbf{a}_1 + \mathbf{a}_2) \cdot \mathbf{k}} \\ e^{-i\mathbf{a}_1 \cdot \mathbf{k}} & 1 & 1 \end{bmatrix},$$

and the momentum sum runs over the folded Brillouin zone (BZ). The nine complex order parameters ξ_{ij} of our mean field decoupling represent the nine bonds in the enlarged unit cell, as pictorially represented in Fig. 1(c). We solve Eq. (2) self-consistently with the constrain imposed by the Luttinger theorem [20], which reads (ignoring logarithmic corrections in fermion number N_e),

$$n + 3 = \frac{N_e}{N} = \frac{1}{N} \sum_{\mathbf{k}, l} n_F[\varepsilon_l(\mathbf{k}), \mu], \qquad (3)$$

where n is the electron density per unit cell relative to half filling (which in our case corresponds to $n = 0$),

$\varepsilon_l(\mathbf{k})$ is the mean field dispersion for the l band, and $n_F[\varepsilon_l(\mathbf{k}), \mu]$ is the Fermi distribution function. From Eq. (3) we get the renormalized chemical potential μ self-consistently.

The phase diagram and the AH phase.— The mean field phase diagram is shown in Fig. 2 where we plot the different phases (defined in the caption) as a function of the interaction strength V in units of the hopping parameter t and the electron density n. The density of states of the Honeycomb lattice has two Van Hove (VH) singularities at energies $E = \pm t$ where the density of states diverges logarithmically. This gives rise in the standard lattice to electronic instabilities, the most prominent being the so called Pomeranchuk instability corresponding to a metallic phase with a deformed Fermi surface breaking the point symmetry of the lattice [21, 22]. In our phase diagram the density varies from $n = 0$ (half filling) to well above the VH filling which with our convention occurs at $n_{VH} = 0.75$. At each point in the phase diagram a mean field Hamiltonian can be extracted which can be seen as a free Hamiltonian with new effective hopping parameters renormalized by the interaction. At low values of V the symmetric phase (S) represents standard graphene with a uniform renormalization of the hopping. Close to half filling for increasing values of V slightly above $V = 2t$ we recover the Kekulé phase (K) described in [8] which evolves to a Pomeranchuk phase (P) through a finite coexistence region (K+P). Our cal-
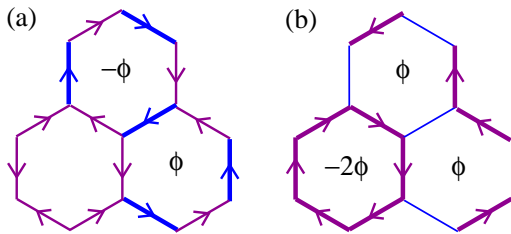
FIG. 3: (color online). Pictorial representation of the order parameters corresponding to the $\mathcal{T}$ broken phases T-I (a) and T-II (b) discussed in the text. The thickness of the bonds represents the modulus of the hopping parameter and the direction of the arrows represents the sign of the phase when it has a complex value. A bond without an arrow means a real hopping.

culation shows that a standard Pomeranchuk instability with an anisotropic renormalization of the hoppings as shown in the inset, is a very robust phase around the VH filling from zero to high values of V. The preferred phase is a nematic one where the C_6 symmetry of the original lattice is broken to a C_2. The inset shows one of the three equivalent configurations oriented along the crystal principal directions. The phase named reduced symmetry (RS) occurring at higher values of the electron density and the interaction is a broken symmetry state with real hopping parameters. The distortion is neither Kekulé type nor Pomeranchuk.

The novel topological Fermi liquid phases appear near $n = 1$. There are two $\mathcal{T}$ broken phases labelled T-I and T-II in Fig. 2 which are the most stable configurations just above the VH filling for moderate values of V beginning at $V \approx 3t$. They are pictorially described in Fig. 3(a) and 3(b), respectively, where the nine complex order parameters of our mean field decoupling are shown. The direction of the arrows represents the sign of the phase of the given complex hopping, and the thickness of the line represents its modulus. The phases can also be understood as patterns of orbital currents. Current conservation at each of the six atoms in the unit cell plus the zero overall flux condition allow for only two independent $\mathcal{T}$ breaking phases, T-I and T-II in our notation, defined by their corresponding flux pattern in the unit cell. We note that in addition of having the non-trivial fluxes described their structure includes a Kekulé distortion of the bonds. The discrete symmetries of the mean field Hamiltonian help to classify the topological properties of a given phase [19]. The phase T-I breaks $\mathcal{T}$ and inversion $\mathcal{I}$, but preserves $\mathcal{TI}$. The T-II breaks $\mathcal{T}$ but $\mathcal{I}$ is preserved. At a given point of the phase diagram the Hall conductivity can be computed from the single particle Bloch states $|\Psi_l(\mathbf{k})\rangle$ associated to the appropriate

mean field Hamiltonian from the expression:

$$\sigma^{ab}(\mu) = \frac{e^2}{\hbar} \frac{1}{N\mathcal{V}} \sum_{k,l} \Omega_l^{ab}(\mathbf{k}) n_F[\varepsilon_l(\mathbf{k}), \mu], \qquad (4)$$

where $\mathcal{V}$ is the volume of the unit cell, and $\Omega_l^{ab}(\mathbf{k})$ is the Berry curvature defined from the Berry connection: $\mathcal{A}_l^a(\mathbf{k}) = -i\left\langle \Psi_l(\mathbf{k})|\nabla_{(\mathbf{k})}^a \Psi_l(\mathbf{k})\right\rangle$, $\Omega_l^{ab}(\mathbf{k}) = \nabla_k^a \mathcal{A}_l^b(\mathbf{k}) - \nabla_k^b \mathcal{A}_l^a(\mathbf{k})$. The T-II phase is of the type II in the classification given in [19]: it breaks $\mathcal{T}$ but preserves $\mathcal{I}$ and the Hall conductivity is generically non zero. The T-I phase, Fig. 3(a), breaks $\mathcal{T}$ and $\mathcal{I}$ but preserves $\mathcal{TI}$ so it corresponds to a $\mathcal{T}$ broken phase of type I and has zero Hall conductivity. We have further confirmed this picture by numerical computation of the Hall conductivity Eq. (4). A plot of the Hall conductivity as a function of the interaction V for different values of the density in the region T-II of the phase diagram is shown in the right hand side of Figure 4.

A very neat analysis of the topological properties of the various metallic phases in the phase diagram can be done by studying the low energy effective bands. We have plotted the mean field band structure of the T-II phase in Fig. 4 obtained for the parameter values $V = 5t$, $n = 1.13$. Focusing on the relevant bands around the Fermi level, it is easy to understand the qualitative behavior of the non vanishing Hall conductivity in this phase. The Fermi level crosses a massive Dirac structure around the Γ point and so there is a non-zero contribution to the AH conductivity of this cone. The non-quantized contribution to the AH conductivity from the cone is given by [24, 25] $\sigma_H = \frac{e^2}{2h} \frac{M(n,V)}{|\tilde{\mu}(n,V)|}$, where $M(n,V)$ is the gap at the Γ point and $\tilde{\mu}(n,V)$ is the renormalized chemical potential relative to the middle of the gap, both of which depend strongly on the parameters of the phase diagram. To better understand the nature of the $\mathcal{T}$ broken phases we note that they arise in the region of the parameter space close to the density where there are four electrons per unit cell: $n = 1$. This is a very special filling: Not only it is commensurate with the lattice, but it enhances the formation of current loops self-consistently maintained at each hexagon following the configurations shown in Fig. 3. In the $\mathcal{T}$ broken part of the phase diagram, along the line $n = 1$ the system becomes an insulator. The band structure near the Fermi level is similar to the one shown in Fig. 4 left but the cones are further apart and the Fermi level lies in the gap. Away from this line we have the situation described before. The majority of the electrons will still form currents as these in Fig. 3 and the excess (defect) electrons are responsible for the metallicity of the system.

Discussion and future.— Part of the physics discussed in this work can be tested in actual graphene samples. The simple deformation of the Fermi surface pointing to a Pomeranchuk instability is a very robust phase that may
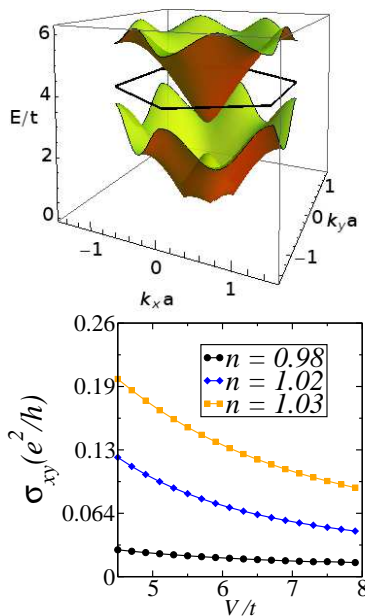
FIG. 4: (color online). (Left) Two lowest energy bands for the mean field Hamiltonian in the AH phase obtained with $V = 5t$, $n = 1.13$. The hexagonal line marks the position of the Fermi level. (Right) The Hall conductivity as a function of V for various electron densities in the T-II regions of the phase diagram. From lower to upper: n=0.98, 1.02, 1.03.

prevail even if other instabilities not considered in this work are allowed. The AH phase can be more difficult to observe in graphene since it occurs at higher values of the interactions but it could potentially be tested in cold atom experiments with optical lattices [26, 27].

Other phases may compete with the ones described in this work when charge decoupling and spin degrees of freedom are included in the system. It will be interesting to see how they compete with the AH phase obtained in this work. In previous studies of similar systems the AH phases evolved to spin Hall phases when spin and the on–site Hubbard interaction U was added [19]. Very appealing possibilities will open in the Pomeranchuk region of the phase diagram in Fig. 2 when spin is included along the lines of [28]. Spin effects have also been explored recently in [29]. A preliminary analysis of the phase transitions shows that they are of first order what ensures its stability at least at the mean field level.

Conclusions.— We have found a spontaneous symmetry breaking to an AH phase in a tight binding model in the Honeycomb lattice with only nearest neighbor hopping parameters and Coulomb interaction. The extra physics required to get such a phase is provided by the folding of the BZ that allows for spontaneous non-zero currents with zero overall magnetic flux to form inside the unit cell generating $\mathcal{T}$ broken phases. The $\mathcal{T}$ broken phase is predominantly an AH metal of the type II in the classification given in [19] where the interaction V gives

rise to orbital currents together with a Kekulé distortion.

The findings of this work open a whole set of possibilities for new realization of exotic phases based on lattice models. Enlarging the unit cell is a very simple procedure that increases enormously the phase space of any given lattice. This is exemplified in the model studied here where in addition to the AH phase we have found a very rich phase diagram even when neglecting spin and charge density wave instabilities.

[1] Z. F. Ezawa, *Quantum Hall Effects - Field Theoretical Approach and Related Topics* (World Scientific, Singapore, 2008).
[2] N. Nagaosa, J. Sinova, S. Onoda, A. H. MacDonald, and N. P. Ong, Rev. Mod. Phys. **82**, 1539 (2010).
[3] G. E. Volovik, *The universe in a helium droplet* (Clarendon Press, Oxford, 2003).
[4] F. D. M. Haldane, Phys. Rev. Lett. **61**, 2015 (1988).
[5] F. Guinea, M. I. Katsnelson, and A. G. Geim, Nature Physics **6**, 30 (2010).
[6] M. Z. Hasan and C. L. Kane, Rev. Mod. Phys. **82**, 3045 (2010).
[7] F. D. M. Haldane, Phys. Rev. Lett. **93**, 206602 (2004).
[8] C.-Y. Hou, C. Chamon, and C. Mudry, Phys. Rev. Lett. **98**, 186809 (2007).
[9] M. Franz, Physics **3**, 24 (2010).
[10] A. A. Nersesyan, Phys. Lett. A **153**, 49 (1991).
[11] E. H. Lieb, Phys. Rev. Lett. **73**, 2158 (1994).
[12] S. Chakravarty, R. B. Laughlin, D. K. Morr, and C. Nayak, Phys. Rev. B **63**, 094503 (2001).
[13] C. M. Varma, Phys. Rev. B **73**, 155113 (2006).
[14] K. Sun, H. Yao, E. Fradkin, and S. A. Kivelson, Phys. Rev. Lett. **103**, 046811 (2009).
[15] S. Raghu, X.-L. Qi, C. Honerkamp, and S.-C. Zhang, Phys. Rev. Lett. **100**, 156401 (2008).
[16] T. Pereg-Barnea and G. Refael, arXiv:1011.5243 (2010).
[17] J. Wen, A. Ruegg, C.-C. J. Wang, and G. A. Fiete, Phys. Rev. B **82**, 075125 (2010).
[18] Z. Qiao et al., Physical Review B **82**, 161414(R) (2010).
[19] K. Sun and E. Fradkin, Phys. Rev. B **78**, 245122 (2008).
[20] J. M. Luttinger, Phys. Rev. **119**, 1153 (1960).
[21] B. Valenzuela and M. A. H. Vozmediano, New J. Phys. **10**, 113009 (2008).
[22] C. Lamas, D. Cabra, and N. Grandi, Phys. Rev. B **80**, 075108 (2009).
[23] J. Mañes, F. Guinea, and M. A. H. Vozmediano, Phys. Rev. B **75**, 155424 (2007).
[24] C. Kane and E. Mele, Phys, Rev. Lett. **95**, 146802 (2005).
[25] A. Cortijo, A. G. Grushin, and M. A. H. Vozmediano, Phys. Rev. B **82**, 195438 (2010).
[26] L. B. Shao, S.-L. Zhu, L. Sheng, D. Y. Xing, and Z. D. Wang, Phys. Rev. Lett. **101**, 246810 (2008).
[27] K. L. Lee, B. Gremaud, R-Han, B.-G. Englert, and

C. Miniatura, Phys. Rev. A **80**, 043411 (2009).

[28] C. Wu, K. Sun, E. Fradkin, and S. C. Zhang, Phys. Rev. B **75**, 115103 (2007).

[29] T. Li, arXiv:1103.2420 (2011).